Hiroki Yamada, MD
Yoshio Koshimoto, MD
Norihiro Sadato, MD
Yukio Kawashima, RT
Masato Tanaka, RT
Chika Tsuchida, MD
Masayuki Maeda, MD
Yoshiharu Yonekura, MD
Yasushi Ishii, MD

Index terms:
Blood, flow dynamics, 153.12112, 153.121412, 17.12112, 17.121412
Brain, blood flow, 10.12144, 10.919, 153.919
Brain, infarction, 10.78
Brain, perfusion, 10.12144, 10.919, 153.919
Magnetic resonance (MR), perfusion study, 153.12112

Radiology 1999; 210:558–562

Abbreviations:
GRE = gradient-echo
RARE = rapid acquisition with relaxation enhancement
SE = spin-echo

[1] From the Department of Radiology (H.Y., Y.Koshimoto, M.T., C.T., M.M., Y.I.) and Biomedical Imaging Research Center (N.S., Y.Y.), Fukui Medical University, 23 Shimoaizuki, Matsuoka, Yoshida, Fukui, 910-11, Japan, and the Department of Radiology, Obama Hospital, Fukui, Japan (Y.Kawashima). Received March 5, 1998; revision requested May 6; revision received May 28; accepted August 10. Address reprint requests to H.Y.

Author contributions:
Guarantor of integrity of entire study, H.Y.; study concepts, Y.I.; study design, Y.Y.; definition of intellectual content, H.Y.; literature research, H.Y.; clinical studies, C.T.; experimental studies, H.Y.; data acquisition, H.Y., Y.Kawashima; data analysis, Y.Koshimoto, Y.Kawashima; statistical analysis, M.T.; manuscript preparation and editing, N.S.; manuscript review, M.M.

Crossed Cerebellar Diaschisis: Assessment with Dynamic Susceptibility Contrast MR Imaging[1]

The authors investigated the feasibility of using T2-weighted, half-Fourier rapid acquisition with relaxation enhancement, or RARE, dynamic susceptibility contrast magnetic resonance (MR) imaging to depict crossed cerebellar diaschisis. In 10 patients after unilateral supratentorial stroke, crossed cerebellar diaschisis was demonstrated in the relative regional cerebellar blood volume maps obtained with MR imaging. Cerebellar blood volume values for the nonaffected cerebellar hemisphere were significantly larger than those for the affected side (P = .0003).

Crossed cerebellar diaschisis is metabolic depression in the cerebellum contralateral to supratentorial lesions (1). To our knowledge, it was first described in a positron emission tomography (PET) study conducted by Baron et al (2) in 1980. Crossed cerebellar diaschisis is interpreted as functional deactivation, presumably caused by a loss of excitatory or inhibitory afferent inputs on the corticopontocerebellar or other pathways (1,2). This phenomenon has been repeatedly described in studies of oxygen consumption (1), cerebellar blood flow (3), and glucose metabolism (4), essentially by using imaging techniques with radioisotopes (5–13). Yamauchi et al (11) found that the crossed cerebellar hypoperfusion correlated with cerebral oxygen metabolism of the affected side but not with blood flow. Hence, assessment of crossed cerebellar diaschisis may be used to estimate the relative uncoupling between blood flow and metabolism (misery perfusion) from a single blood flow study. However, to our knowledge, the detection of crossed cerebellar diaschisis by means of magnetic resonance (MR) imaging has not been reported.

Dynamic susceptibility contrast MR imaging has been used to demonstrate cerebral hemodynamics (14–17). Half-Fourier rapid acquisition with relaxation enhancement (RARE) (HASTE; Siemens Medical Systems, Iselin, NJ) is a high-speed, heavily T2-weighted sequence with echo train length of 128 that is performed in approximately 1–2 sec (18–22). The change in signal intensity depicted with this sequence in dynamic susceptibility contrast MR imaging is supposed to reflect microvascular hemodynamics (23–25). The purpose of this study was to investigate the feasibility of using half-Fourier RARE, dynamic susceptibility contrast MR imaging to depict crossed cerebellar diaschisis in patients after unilateral supratentorial stroke.

Materials and Methods

We studied 10 patients (six men and four women; age range, 48–65 years; mean age, 60.8 years) after unilateral supratentorial stroke (Table) and eight age-matched healthy control subjects (four men and four women; age range, 42–63 years; mean age, 53.5 years) who had no cerebrovascular lesions. The study protocol was approved by the institutional ethical committee, and all patients and control subjects gave their written informed consent.

A 1.0-T superconducting MR imaging system (Magnetom Impact; Siemens) was used to acquire fast spin-echo (SE) T2-weighted images before the administration of the contrast agent (repetition time msec/echo time msec = 3,000/90; section thickness, 5 mm; field of view, 21 cm; matrix, 256 × 192).

T2-weighted dynamic susceptibility contrast MR imaging was performed with

Patient Data

Patient No./ Sex/Age (y)	Lesion Location*	No. of Days after Onset of Symptoms	Relative Regional Cerebellar Blood Volume	
			Affected Side	Nonaffected Side
1/M/60	Right MCA infarction	38	11.0	13.7
2/F/78	Right MCA infarction	14	11.1	13.7
3/F/68	Right MCA infarction	20	9.0	11.0
4/M/64	Left BG hemorrhage	14	10.9	12.0
5/M/37	Left MCA infarction	6	7.8	11.6
6/M/48	Left MCA infarction	13	8.3	8.9
7/F/55	Right BG hemorrhage	25	11.1	13.7
8/F/70	Left MCA infarction	42	15.3	16.9
9/M/62	Right BG hemorrhage	54	5.2	6.3
10/M/66	Left MCA infarction	120	8.0	8.7

* BG = basal ganglia, MCA = middle cerebral artery.

a half-Fourier RARE sequence (18) (3,000/87; flip angle, 90°; field of view, 210 mm; section thickness, 10 mm; matrix, 128 × 256). A half-Fourier algorithm was used to reconstruct the images (19–22). A 20-gauge intravenous needle was inserted into the vein of the right antecubital fossa and maintained for the duration of the study. After three images were obtained, a bolus injection of 0.15 mmol per kilogram of body weight gadopentetate dimeglumine (Magnevist; Schering, Berlin, Germany) was administered and followed by a 20-mL saline solution flush. Imaging time was 3 seconds per image with no interimage delay; a total of 30 images were obtained. The T2-weighted dynamic images were obtained at the same coronal location where the volume of cerebellar hemisphere was the largest (Figure, part a). The participant's head was fixed in the head coil with sponges, and visual inspection revealed no apparent misregistration of the dynamic images.

Rosen et al (15) empirically determined that the relationship between the signal change, T2* rate change (ΔR2*), and brain tissue concentration of the contrast agent (C) is expressed by a single exponential expression: $S_i = S_0 e^{-TE(\Delta 1/T2^*)}$, $-\ln(S_i/S_0)/TE = \Delta R2^*$, $\Delta R2^* = k(C)$, where S_0 is the precontrast signal intensity, S_i is the signal intensity at time i after injection of gadopentetate dimeglumine, TE is echo time, and k is a tissue-specific constant. The raw signal intensity–time series data are converted to concentration-time data by means of this relationship. The area under the concentration-time curve is proportional to the local blood volume (15). The map of the relative regional cerebellar blood volume was calculated as the sum of the first-pass T2 rate change (ΔR2) images calculated on a pixel-by-pixel basis ($\Delta R2 = -\ln(S_i/S_0)/TE$, where i is time. Areas with decreased signal intensity on the relative regional cerebellar blood volume map indicate decreased relative regional cerebellar blood volume, and these images were used for visual evaluation.

More quantitative evaluation of the relative regional cerebellar blood volume was performed by selecting regions of interest in the bilateral cerebellum. We made the region of interest as large as possible in the cerebellar hemisphere (Figure, part b). A gamma variate function was fitted to the ΔR2 time curves from these regions of interest, and relative regional cerebellar blood volume was determined as the area under the curve. All relative regional cerebellar blood volume values in 36 regions of interest in all participants were obtained by means of reliable gamma variate fitting analysis (r, 0.95–0.98; $P < .001$). The paired t test was used to analyze the difference in relative regional cerebellar blood volume of the cerebellar cortex ipsilateral and contralateral to the cerebral lesion in patients and of the right and left cerebellar hemisphere in control subjects. From the relative regional cerebellar blood volume value, we calculated the interhemispheric asymmetry index (IAI) between the contralateral (CL) and the ipsilateral (IL) cerebellar hemisphere in the patients as IAI = (IL − CL)/IL × 100. We also calculated the interhemispheric asymmetry index between the right (R) and left (L) cerebellar hemispheres in control subjects as IAI = $|R - L|/(R + L) \times 200$. In the patients, the crossed cerebellar diaschisis was defined as statistically significant when the value of the interhemispheric asymmetry index exceeded that of the control value (mean ± 2 SD) as derived from the control subjects (8,11).

Results

In the patients, conventional fast SE, T2-weighted images revealed no morphologic alterations, including crossed cerebellar atrophy, in the cerebellum. Signal intensity change from larger vessels in the cerebellar cortex are not prominent in the dynamic T2* rate change images (Figure, part c).

In eight patients (patients 1–5 and 7–9), the relative regional cerebellar blood volume maps showed crossed cerebellar hypoperfusion as relatively dark areas in the contralateral cerebellar hemisphere (affected side) compared with the ipsilateral hemisphere (nonaffected side), with complete agreement between three readers (Figure, part d). In all 10 patients, the relative regional cerebellar blood volume values of the nonaffected cerebellar hemisphere were significantly larger than those of the affected side ($P = .0003$, 9 df, paired t test). There was no significant difference in relative regional cerebellar blood volume between the right and left cerebellar hemispheres in control subjects ($P = .83$, 7 df, paired t test). The interhemispheric asymmetry index (mean ± SD) was 4.1 ± 2.3 in control subjects and 16.0 ± 7.9 in patients. Statistically significant asymmetry in relative regional cerebellar blood volume was observed in eight patients (ie, individual interhemispheric asymmetry index was greater than 8.6%, the confidence limit in the control subjects).

Discussion

In this study, we evaluated a dynamic susceptibility contrast MR imaging technique with a heavily T2-weighted, SE-based half-Fourier RARE sequence. The half-Fourier RARE sequence creates a series of echoes by applying a 90° excitation pulse followed by a train of refocusing pulses. A half-Fourier algorithm is used to reconstruct the images (18–22). Because the images are reconstructed sequentially, the time needed to acquire an image is proportional to the echo train length and the echo spacing, and with the parameters we used, was 1,000 msec. Half-Fourier RARE is a natural extension of known turbo or fast SE sequences (26). After each section is excited, as many as 128 echoes are generated with a 180° pulse. Each of these echoes is phase encoded individually. Owing to the nature of the 180° pulse, the susceptibility effect is minimized. Local field inhomogeneity and susceptibility artifacts from adjacent

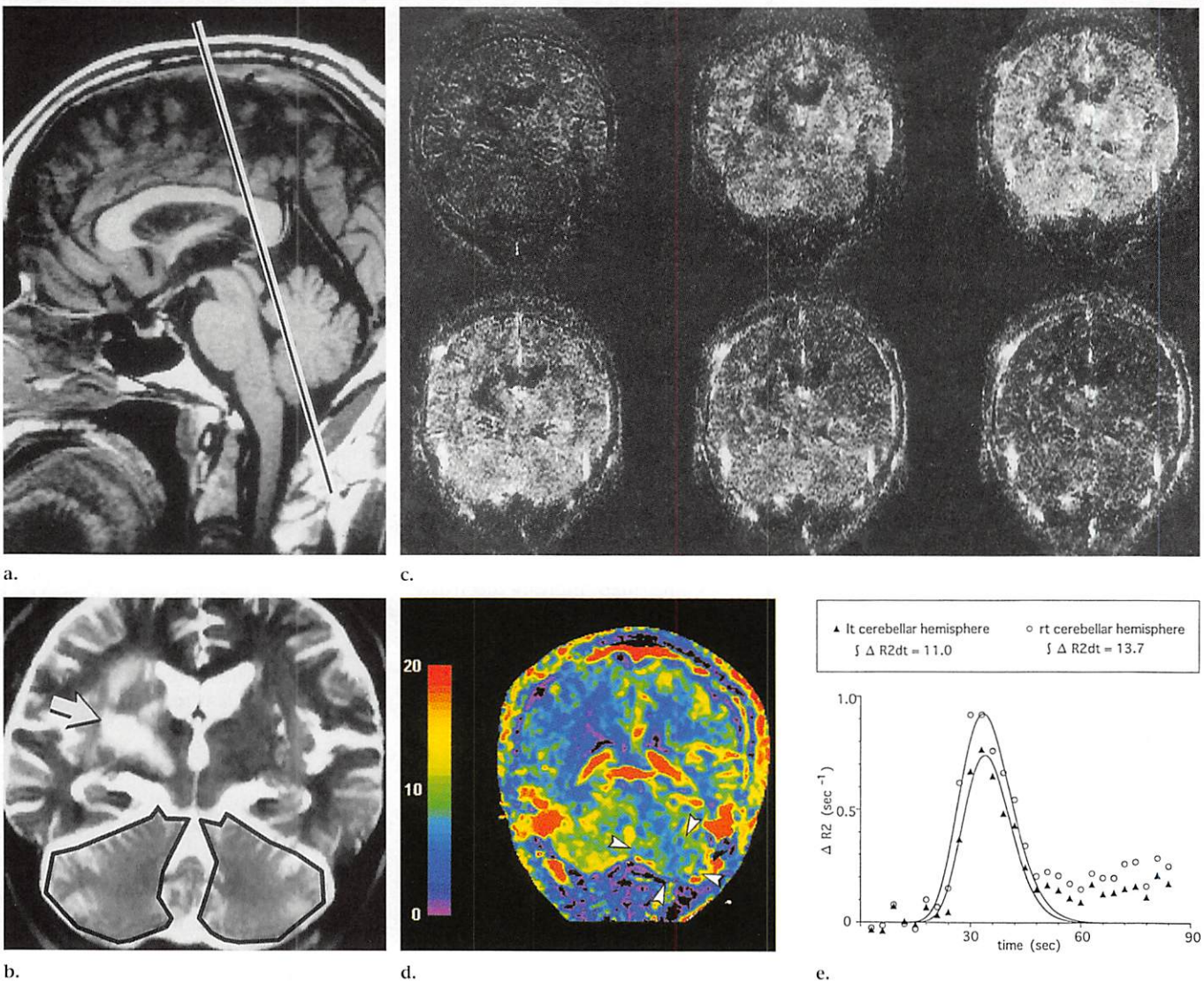

Patient 1. Images obtained after cerebral infarction in the right corona radiata. **(a)** Sagittal T1-weighted image obtained to select the section location (line) for a coronal half-Fourier RARE image. **(b)** Original coronal half-Fourier RARE image for dynamic susceptibility contrast MR imaging. T2-weighted half-Fourier RARE image shows an area of high signal intensity (arrow) in the right corona radiata, which indicates cerebral infarction. The black lines in the bilateral cerebellar hemispheres outline the regions of interest for the T2* rate change–time curves. **(c)** Top left to bottom right: Six sequential calculated images display T2* rate change values after administration of contrast material. Note that T2* rate changes from larger vessels in the cerebellar cortex are not prominent. **(d)** Map of the relative regional cerebellar blood volume. There is an area of crossed cerebellar hypoperfusion (arrowheads) in the left cerebellar cortex. **(e)** T2 rate change ($\Delta R2$)–time curves (with gamma variate fit) measured in a region of interest in the right (*rt*) and left (*lt*) cerebellar hemispheres show a decrease in relative regional cerebellar blood volume ($\int \Delta R2dt$), determined as the area under the curve, in the affected left cerebellar hemisphere compared with that in the nonaffected right side.

mastoid air cells and paranasal sinuses contribute to degradation of the image quality of the cerebellum on conventional T2*-weighted gradient-echo (GRE) and echo-planar images. Because of the low susceptibility of half-Fourier RARE to artifact, image degradation of the cerebellar hemisphere is effectively eliminated compared with T2*-weighted images.

The most important difference between the half-Fourier RARE sequence and conventional GRE–based T2*-weighted dynamic susceptibility contrast MR imaging is that the former reflects volume changes in the capillary vessels. Ogawa et al (27) reported that the diffusion-independent dephasing effects observed at large radii are absent on SE images but not on GRE images. For small vessels, averaging of the field by diffusion is extensive; therefore, the difference between GRE and SE imaging is small. Weisskoff et al (23) and Boxerman et al (24) simulated the microscopic susceptibility variations in SE (T2-weighted) and GRE (T2*-weighted) imaging. Findings with their simulation suggested that SE and GRE imaging are sensitive to different sized blood vessels. Since SE relaxivity peaks for vessel size at or below capillary size, they expected the SE imaging to weight more heavily contrast within the capillary blood volume, whereas blood volume measured with GRE imaging approximates the total blood volume, including supplying arteries and draining veins, as do all the other tomographic blood volume techniques.

T2 weighting may occur strongly within the large vessels, where the large-vessel

blood volume is a statistically significant fraction of the voxel volume. However, with T2-weighted dynamic susceptibility contrast MR imaging, the intravascular component from larger vessels is generally neglected because the bulk of the blood volume, which is only 1%–3% of the total brain volume, is in small vessels such as the capillaries and venules. Hence, the models are essentially based on extravascular volume. In the present study, this is safely assumed because the regions of interest used for assessment of crossed cerebellar diaschisis are relatively large.

It is well established that the energy-dependent change in neuronal function, particularly in synaptic activity, and blood flow are coupled (28). Changes in regional cerebellar blood flow are known to exceed changes in regional cerebellar blood volume by two to four times (29). This may indicate that change in capillary blood volume is more tightly coupled with change in regional cerebellar blood flow than change in total blood volume. This speculation is reasonable, as the capillaries are responsible for delivery of substrate to tissues. Hence, measurement of regional cerebellar blood volume with half-Fourier RARE may reflect changes in regional cerebellar blood flow, and hence, neuronal activity, more sensitively than changes in total blood volume (23,24). Therefore, we adopted T2-weighted half-Fourier RARE imaging to evaluate functional hemodynamic information in crossed cerebellar diaschisis.

Findings in the present study show a high incidence of crossed cerebellar diaschisis (eight of 10 patients) in unilateral supratentorial stroke. Although the number of patients is small, this finding is consistent with findings in other PET studies. In a PET study of cerebral oxygen consumption by Miura et al (8), 31 of 35 patients with unilateral cerebral infarction in the territory of the middle cerebral artery had crossed cerebellar diaschisis. Further, findings in a PET study of regional cerebellar blood flow by Yamauchi et al (11) showed crossed cerebellar diaschisis in 16 of 24 patients with unilateral supratentorial stroke. Thus, findings in these studies support the effectiveness of half-Fourier RARE dynamic susceptibility contrast MR imaging in depicting crossed cerebellar diaschisis.

The advantage of depicting changes in capillary blood volume rather than in total cerebellar blood volume in crossed cerebellar diaschisis is supported by findings in the study of Yamauchi et al (11). They used PET to evaluate regional cerebellar blood flow, rate of oxygen metabolism, oxygen extraction fraction, and blood volume in the cerebellar cortex in patients with unilateral supratentorial stroke. They found that the cerebellar blood volume decreased, with a normal ratio of cerebellar blood flow to cerebellar blood volume in patients with crossed cerebellar diaschisis. The proportional decrease in cerebellar blood volume and cerebellar blood flow is crucial to differentiating a deafferentiation-induced reduction in cerebellar blood flow from an ischemic condition in morphologically normal brain areas. From these results, they suggested that primary metabolic suppression from deafferentiation causes vasoconstriction, resulting in reduced cerebellar blood volume.

The half-Fourier RARE dynamic susceptibility contrast MR imaging technique has some limitations compared with PET, single photon emission tomography (SPECT), and other perfusion techniques such as single section limitation, relative assessment of the cerebellar blood volume, and contrast agent requirement. Further improvement in the temporal resolution with the half-Fourier RARE technique will enable performance of multisection half-Fourier RARE dynamic susceptibility contrast MR imaging, and the quantitative assessment of cerebellar blood volume to cerebellar blood flow, since this would allow determination of the arterial input function (30). A flow-sensitive nonenhanced perfusion technique—such as echo-planar imaging and signal targeting with alternating radio frequency, or EPISTAR (31), or flow-sensitive alternating inversion recovery, or FAIR (32)—could assess crossed cerebellar diaschisis as half-Fourier RARE methods do, although no report is yet available, to our knowledge. The former may suffer from the inherent susceptibility artifact particularly in the infratentorial regions, unavailability of quantification, and limitation of the number of sections. The latter may quantify cerebellar blood flow, but the signal-to-noise ratio is relatively low.

In conclusion, findings in the present study showed that the relative regional cerebellar blood volume map obtained with T2-weighted, half-Fourier RARE, dynamic susceptibility contrast MR imaging successfully depicted crossed cerebellar diaschisis in patients with supratentorial stroke. Its clinical feasibility might be confirmed by means of direct comparison with findings at PET or SPECT in a larger population.

References

1. Pantano P, Baron JC, Samson Y, Bousser MG, Derouesne C, Comar D. Crossed cerebellar diaschisis: further studies. Brain 1986; 109:677–694.
2. Baron JC, Bousser MG, Comar D, Castaigne P. Crossed cerebellar diaschisis in human supratentorial brain infarction. Trans Am Neurol Assoc 1980; 105:459–461.
3. Meneghetti G, Vorstrup S, Mickey B, Lindewald H, Lassen NA. Crossed cerebellar diaschisis in ischemic stroke: a study of regional cerebral blood flow by ^{133}Xe inhalation and single photon emission computerized tomography. J Cereb Blood Flow Metab 1984; 4:235–240.
4. Alavi A, Mirot A, Newberg A, et al. Fluorine-18-FDG evaluation of crossed cerebellar diaschisis in head injury. J Nucl Med 1997; 38:1717–1720.
5. Brott TG, Gelfand MJ, Williams CC, Spilker JA, Hertzberg VS. Frequency and patterns of abnormality detected by iodine-123 amine emission CT after cerebral infarction. Radiology 1986; 158:729–734.
6. Broich K, Hartmann A, Biersack HJ, Horn R. Crossed cerebello-cerebral diaschisis in a patient with cerebellar infarction. Neurosci Lett 1987; 83:7–12.
7. Pantano P, Lenzi GL, Guidetti B, et al. Crossed cerebellar diaschisis in patients with cerebral ischemia assessed by SPECT and 123I-HIPDM. Eur Neurol 1987; 27: 142–148.
8. Miura H, Nagata K, Hirata Y, Satoh Y, Watahiki Y, Hatazawa J. Evolution of crossed cerebellar diaschisis in middle cerebral artery infarction. J Neuroimaging 1994; 4:91–96.
9. Tanaka M, Kondo S, Hirai S, Ishiguro K, Ishihara T, Morimatsu M. Crossed cerebellar diaschisis accompanied by hemiataxia: a PET study. J Neurol Neurosurg Psychiatry 1992; 55:121–125.
10. Fulham MJ, Brooks RA, Hallett M, Di Chiro G. Cerebellar diaschisis revisited: pontine hypometabolism and dentate sparing. Neurology 1992; 42:2267–2273.
11. Yamauchi H, Fukuyama H, Kimura J. Hemodynamic and metabolic changes in crossed cerebellar hypoperfusion. Stroke 1992; 23:855–860.
12. Sakashita Y, Matsuda H, Kakuda K, Takamori M. Hypoperfusion and vasoreactivity in the thalamus and cerebellum after stroke. Stroke 1993; 24:84–87.
13. Fulham MJ, Dietz MJ, Duyn JH, Shih HH, Alger JR, Di Chiro G. Transsynaptic reduction in *N*-acetyl-aspartate in cerebellar diaschisis: a proton MR spectroscopic imaging study. J Comput Assist Tomogr 1994; 18:697–704.
14. Belliveau JW, Rosen BR, Kantor HL, et al. Functional cerebral imaging by susceptibility-contrast NMR. Magn Reson Med 1990; 14:538–546.
15. Rosen BR, Belliveau JW, Chien D. Perfusion imaging by nuclear magnetic resonance. Magn Reson Q 1989; 5:263–281.
16. Rosen BR, Belliveau JW, Buchbinder BR, et al. Contrast agents and cerebral hemodynamics. Magn Reson Med 1991; 19:285–292.
17. Belliveau JW, Kennedy DN Jr, McKinstry RC, et al. Functional mapping of the human visual cortex by magnetic resonance imaging. Science 1991; 254:716–719.
18. Kiefer B, Grassner J, Haussmann R. Image acquisition in a second with a half-Fourier-acquisition single-shot turbo spin echo. JMRI 1994; 4(suppl):86–87.

19. Aerts P, Van Hoe L, Bosmans H, Oyen R, Marchal G, Baert AL. Breath-hold MR urography using the HASTE technique. AJR 1996; 166:543–545.
20. Regan F, Smith D, Khazan R, et al. MR cholangiography in biliary obstruction using half-Fourier acquisition. J Comput Assist Tomogr 1996; 20:627–632.
21. Levine D, Hatabu H, Gaa J, Atkinson MW, Edelman RR. Fetal anatomy revealed with fast MR sequences. AJR 1996; 167:905–908.
22. Miyazaki T, Yamashita Y, Tsuchigame T, Yamamoto H, Urata J, Takahashi M. MR cholangiopancreatography using HASTE (half-Fourier acquisition single-shot turbo spin-echo) sequences. AJR 1996; 166: 1297–1303.
23. Weisskoff RM, Zuo CS, Boxerman JL, Rosen BR. Microscopic susceptibility variation and transverse relaxation: theory and experiment. Magn Reson Med 1994; 31: 601–610.
24. Boxerman JL, Hamberg LM, Rosen BR, Weisskoff RM. MR contrast due to intravascular magnetic susceptibility perturbations. Magn Reson Med 1995; 34:555–566.
25. Constable RT, Kennan RP, Puce A, McCarthy G, Gore JC. Functional NMR imaging using fast spin echo at 1.5 T. Magn Reson Med 1994; 31:686–690.
26. Henning J, Nauerth A, Friedburg H. RARE imaging: a fast imaging method for clinical MR. Magn Reson Med 1986; 823–833.
27. Ogawa S, Menon RS, Tank DW, et al. Functional brain mapping by blood oxygenation level–dependent contrast magnetic resonance imaging: a comparison of signal characteristics with a biophysical model. Biophys J 1993; 64:803–812.
28. Raichle ME. Circulatory and metabolic correlates of brain function in normal humans. In: Mountcastle VB, Plum F, Geiger SR, eds. Handbook of physiology. New York, NY: Oxford University Press, 1987; 643–674.
29. Grubb RL Jr, Raichle ME, Eichling JO, Ter Pogossian MM. The effects of changes in $Paco_2$ on cerebral blood volume, blood flow, and vascular mean transit time. Stroke 1974; 5:630–639.
30. Rempp KA, Brix G, Wenz F, Becker CR, Guckel F, Lorenz WJ. Quantification of regional cerebral blood flow and volume with dynamic susceptibility contrast-enhanced MR imaging. Radiology 1994; 193:637–641.
31. Edelman RR, Siewert B, Darby DG, et al. Qualitative mapping of cerebral blood flow and functional localization with echo-planar MR imaging and signal targeting with alternating radio frequency. Radiology 1994; 192:513–520.
32. Kim SG, Tsekos NV. Perfusion imaging by a flow-sensitive alternating inversion recovery (FAIR) technique: application to functional brain imaging [published erratum appears in Magn Reson Med 1997; 37:675]. Magn Reson Med 1997; 37:425–435.